ACS chemical biology

Articles

pubs.acs.org/acschemicalbiology

Tuning the Affinity of Anion Binding Sites in Porin Channels with Negatively Charged Residues: Molecular Details for OprP

Niraj Modi,[†,§] Iván Bárcena-Uribarri,[†,§] Manjeet Bains,[‡] Roland Benz,[†] Robert E. W. Hancock,[‡] and Ulrich Kleinekathöfer*[,†]

[†]School of Engineering and Science, Jacobs University Bremen, Campus Ring 1, 28759 Bremen, Germany

[‡]Centre for Microbial Diseases and Immunity Research, Department of Microbiology and Immunology, University of British Columbia, Vancouver, British Columbia V6T 1Z4, Canada

Supporting Information

ABSTRACT: The cell envelope of the Gram negative opportunistic pathogen *Pseudomonas aeruginosa* is poorly permeable to many classes of hydrophilic molecules including antibiotics due to the presence of the narrow and selective porins. Here we focused on one of the narrow-channel porins, that is, OprP, which is responsible for the high-affinity uptake of phosphate ions. Its two central binding sites for phosphate contain a number of positively charged amino acids together with a single negatively charged residue (D94). The presence of this negatively charged residue in a binding site for negatively charged phosphate ions is highly surprising due to the potentially reduced binding affinity. The goal of this study was to better understand the role of D94 in phosphate binding, selectivity, and transport using a combination of mutagenesis, electrophysiology, and free-energy calculations. The presence of a negatively charged residue in the binding site is critical for this specific porin OprP as emphasized by the evolutionary conservation of such negatively charged residue in the binding site of several anion-selective porins. Mutations of D94 in OprP to any positively charged or neutral residue increased the binding affinity of phosphate for OprP. Detailed analysis indicated that this anionic residue in the phosphate binding site of OprP, despite its negative charge, maintained energetically favorable phosphate binding sites in the central region of the channel and at the same time decreased residence time thus preventing excessively strong binding of phosphate that would oppose phosphate flux through the channel. Intriguingly mutations of D94 to positively charged residues, lysine and arginine, resulted in very different binding affinities and free energy profiles, indicating the importance of side chain conformations of these positively charged residues in phosphate binding to OprP.

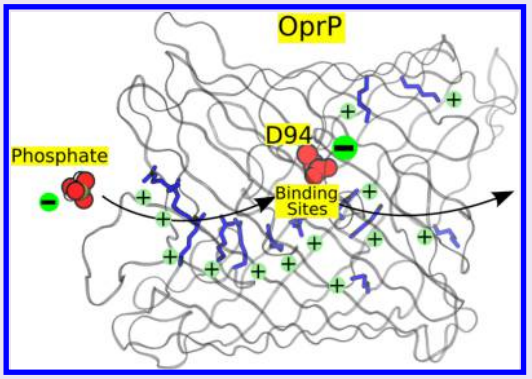

Molecular recognition is a fundamental process underlying all of the critical processes in biology. Enzyme catalysis, transport, immunity, cellular signaling, protein−protein association, the regulation of transcription and translation, as well as the fidelity of DNA replication, among others, rely on recognition between two or more molecular binding partners.[1] It is of key importance to understand how these molecules recognize each other and to investigate the underlying forces that govern these processes. The idea of molecular recognition started from the shape-complementarities based on a "lock-and-key" model as proposed by Fischer to explain enzyme catalysis.[2] Subsequently Pauling and Delbrück postulated in 1940 that intermolecular electrostatic interactions, van der Waals interactions and hydrogen bonds dictate the molecular recognition processes,[3] although the consequences of binding are usually that the binding surfaces are altered, a process termed "induced fit".[4] Since then such intermolecular forces have been investigated not only to understand molecular recognition processes, and the consequences to important (downstream) biological events, but also to enable engineering of such processes for various applications, for example, to optimize intermolecular interactions between protein and ligand to rationally design drug molecules, enhance the activities of enzymes in biotechnology, or change the ion selectivity properties of membrane channels and porins. Our investigations of a phosphate channel from the outer membrane of *Pseudomonas aeruginosa* led us to investigate the possible basis for evolutionary selection of a negatively charged residue in the binding site that would be proposed to decrease binding affinity for anionic phosphate. Here we demonstrated that such a residue is suited to a transport channel since it decreased residence time of phosphate in the binding site, favoring phosphate flux through the channel.

Ion selectivity of membrane proteins represents a prime example of molecular recognition processes. For example, the ability of potassium channels to selectively recognize K^+ over Na^+ is intriguing.[5] Similarly, the ability of a phosphate-selective channel to differentiate between two tetrahedral-shaped

Received: May 20, 2014
Accepted: October 21, 2014
Published: October 21, 2014

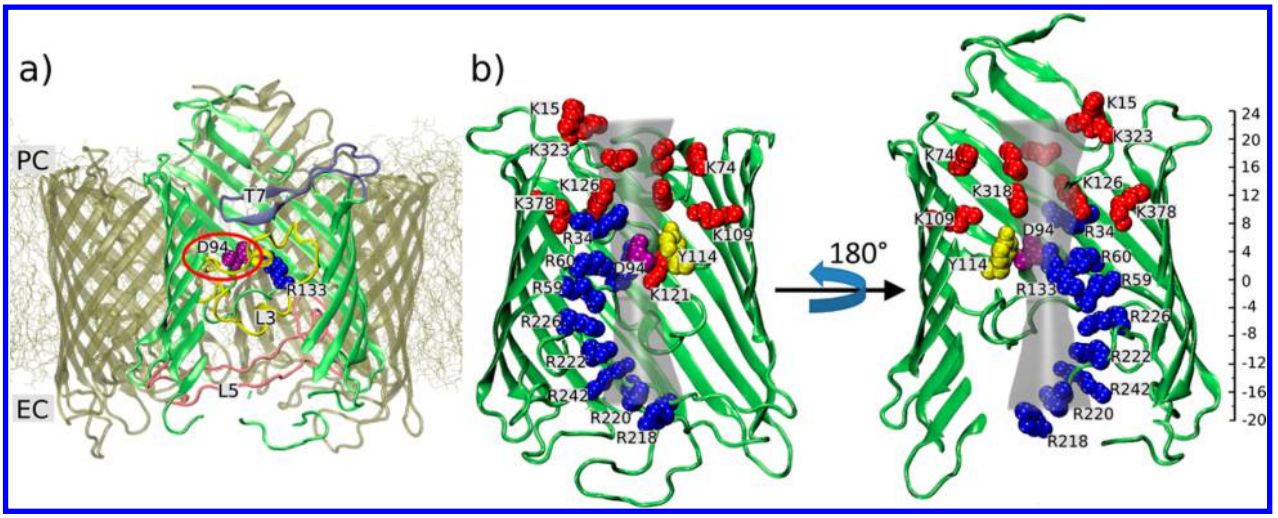

Figure 1. Structural features of OprP. (a) An OprP trimer is shown embedded in a membrane. Important loops, L3, L5, and T7, which are responsible for the formation of narrow regions inside the pore, are shown in one monomer. EC and PC denote the extracellular and periplasmic sides of the pore, respectively. (b) The monomer pore is shown together with a gray hourglass shape to demonstrate the approximate radius of the pore in the different regions and to indicate a possible ion permeation pathway. Important residues, including Asp94 (purple), are labeled and mapped to their position along the *z* axis. Adapted from ref 20.

oxyanions, that is, phosphate and sulfate,[6] is another example of a high-level specificity observed in molecular recognition processes. Compared with globular proteins, molecular recognition in membrane proteins and channels has additional dimensions that need to be considered. Apart from selective permeability toward particular ions or substrates, membrane channels are generally responsible for the efficient and a unidirectional permeation of ions and substrates across the cellular membrane to regulate various biological processes. Efficient permeation, in terms of an appropriate rate of substrate transport across the membrane, requires the channel to have a suitable binding affinity for the permeating substrate, since too strong binding might lead to a very slow permeation. Unidirectional permeation often involves various additional components of the respective transport systems, in addition to a transmembrane channel, which act concertedly to achieve uptake of substrates in the desired direction. An example is the involvement of a periplasmic phosphate binding protein (PBP) to maintain a maximum concentration gradient of free phosphate across the outer membrane and allow vectorial transport of phosphate ions through OprP to the periplasm in *P. aeruginosa*.[7] Phosphate ions first bind to the binding sites within OprP and subsequently to the periplasmic PBP to enable the passage of phosphate ions across the bacterial outer membrane. Such multiple binding partners require appropriate affinities of phosphate for OprP. To achieve such an "appropriate" affinity, a fine-tuning of interactions between the permeating ion and the channel is anticipated. In this study, we focused on the role of the negatively charged aspartate residue of OprP, D94, as an example in regulating such delicate molecular recognition processes in OprP. Electrophysiological bilayer measurements complemented by free energy molecular dynamics simulations provide an ideal platform to probe ion-selective membrane proteins. For example, the KcsA channel[8,9] the NaK channel,[10,11] the ClC channel,[12] and the nicotinic acetylcholine receptor[13] have been investigated in a similar manner to understand their ion selectivity.

OprP is a specific porin that has, in contrast to the so-called general diffusion porins, a binding site for phosphate inside the channel.[18−20] It is induced in the outer membrane of *P. aeruginosa* under phosphate limiting conditions together with a periplasmic phosphate binding protein and an inner membrane transport system.[7,18,20] It is involved in high-affinity uptake of phosphate into the bacterium under such circumstances.[14] Our previous electrophysiological measurements indicated that phosphate binds to OprP with 100−500 times higher binding affinity compared with chloride.[6,15,16] Even more interesting is the 20-fold higher affinity of OprP for phosphate compared with the oxyanion sulfate.[6] In addition to the electrophysiological measurements, we have previously investigated the phosphate selectivity of OprP using free-energy molecular dynamics simulations and explained the possible molecular reasons for the selectivity of the channel.[17] Moreover, Sansom and co-workers probed the selectivity of OprP using molecular dynamics simulations[18] and designed biomimetic nanopores.[19]

The crystal structure of OprP demonstrates a trimeric organization of the specific porin in which each monomer is formed by 16 β-strands that are interconnected via extracellular and periplasmic loops (Figure 1a).[20] Important are the loops L3, L5, and T7 that fold inside the lumen of the pore and form constriction regions inside the channel (Figure 1a). Among important structural features that confer anion selectivity to the channel is the so-called arginine ladder, formed by residues R218, R220, R242, R222, R226, R59, R60, and R34, that extends from the extracellular vestibule down the channel to the middle of the pore (Figure 1b). Another important structural feature is a lysine cluster, consisting of residues K13, K15, K25, K30, K74, K109, K313, K323, and K378, on the periplasmic side of the channel (Figure 1b). Two adjacent central phosphate binding sites are formed by residues D94, R133, Y62, and S125 and by R34 and S124 with residue K121 making contact in one of the three monomers.[17,20]

Recently we showed the importance of the positively charged arginine residue, R133, in the central binding site in determining the phosphate binding affinity of the channel.[21] Both electrophysiological measurements and free-energy molecular dynamics simulations revealed a drastic decrease in binding affinity of phosphate for OprP when R133 was mutated

dx.doi.org/10.1021/cb500399j | *ACS Chem. Biol.* 2015, 10, 441−451

to any other neutral or negatively charged residue. This type of mutant study helps us to understand the relative contribution of each residue in determining the phosphate selectivity of OprP in particular and structure–function relationships of porins in general. Most conserved residues among the orthologs of OprP in *Pseudomonas* species are positively charged arginine and lysine residues. Conservation of important positively charged residues in the anion selective channel with defined binding sites for anions is not very surprising if one considers the complementary nature of the electrostatic interactions between the two binding partners as commonly perceived to be critical in molecular recognition. However, particularly intriguing is the presence of a negatively charged aspartate residue, D94, in one of the central phosphate binding sites. The phosphate ion has two adjacent affinity sites in the central region of the pore, and D94 is part of one of these sites as suggested by both the crystal structure, in which a phosphate ion was clearly evident in the electron density map of OprP, and MD simulations.[17,20] The presence of a negatively charged residue in the binding site of the negatively charged phosphate ions is surprising considering the unfavorable electrostatic interactions between them. Such electrostatic interactions are believed to be very dominant, playing a major role in molecular recognition. For example, the substrate specificities between different subfamilies of aquaporins can be justified based only on the electrostatic profiles of the channels.[22] The functional significance of D94 is also evident because this residue is evolutionarily conserved among OprP orthologs (Supporting Information, Figure S5).

Considering the above observations, we decided to probe the importance of the D94 in the binding and permeation of phosphate ions in or through OprP. A detailed molecular study would potentially yield hints about the role for negatively charged residues, enabling the prospective "design" of anion binding sites for anion selective porins. Different mutants of D94 were generated and investigated using electrophysiological bilayer measurements to determine their effects on phosphate binding affinity. To understand the somewhat surprising results of the experimental studies, free-energy molecular dynamics simulations were performed, aimed at obtaining the molecular reasons behind the experimental observations.

RESULTS

Our initial goal was to understand the relative contribution of the residue D94 in determining the binding affinity of OprP for phosphate. To achieve this, we mutated the negatively charged D94 residue of OprP to the positively charged residues lysine (less bulky compared with R) and arginine (more bulky side chain), as well as neutral residues, asparagine (polar, small side chain compared with Q), glutamine (polar, larger side chain), and alanine (nonpolar, very small side chain). These mutations with amino acids having different physicochemical properties enabled a study of the effect of charge and size of amino acid side chains at the particular position inside the channel in conferring selectivity and the ion transport properties of the channel. We also compared results obtained in the present study with D94 mutant channels with that of our previous studies with the wild-type channel[17] and the R133E mutant channel[21] to enable broader context for explaining the importance of the residue D94 in OprP. R133 is a very important residue in central binding sites and any mutation of this residue led to the drastic decrease in binding affinity of phosphate in OprP.[21]

As shown in Table 1, the stability constants for phosphate-mediated inhibition of chloride transport through the D94 mutants and the corresponding half saturation constant ($1/K$) were highly dependent on the charge, size, and polarity of the residue present in the mutant channels. The highest change in the stability constant was observed for the charge inversion mutant with a smaller side chain, D94K, which resulted in an approximately 30-fold increase in phosphate binding affinity compared with the OprP WT channel. The other charge inversion mutant, D94R, also studied here, also resulted in an increase in phosphate binding affinity as compared with WT but only by about 2-fold, which was initially proposed to relate to the larger size of the arginine side chain compared with that of lysine. We investigated this in more detail below (Figure 3).

Table 1. Single Channel Conductance and Half Saturation Constants of Chloride Conductance Inhibition by Phosphate Binding for WT OprP and D94 Mutants[a]

OprP	G (pS) at $+V$	$1/K^b$ (mM)	K^c (M)
D94 (WT)	160	1.20	820 ± 160
D94K	180	0.042	24000 ± 2000
D94R	160	0.65	1550 ± 250
D94N	280	0.105	9560 ± 1800
D94Q	160	0.52	1910 ± 620
D94A	200	0.27	3700 ± 250
R133E	8	45.0	22 ± 1.8

[a]For comparison, R133E mutant data are also shown (ref 21). The single channel conductance was obtained in 0.1 M KCl, 10 mM MES, pH 6, T = 20 °C, applying 50 mV voltage. The half saturation and stability constants for inhibition by phosphate of Cl^- conductance was obtained from titration experiments as shown in Figure S3, Supporting Information, and using either the Michaelis–Menten equation or the Langmuir equation as described elsewhere.[15,21,23] The phosphate solution had a pH of 6 and was largely monobasic. The mean values (±SD) of at least three individual titration experiments are shown. [b]Half saturation constants for inhibition of chloride conductance by phosphate. [c]Stability constants for inhibition of chloride conductance by phosphate.

Compared with wild-type OprP, mutation of D94 to neutral residues (N, Q, and A) resulted in stronger binding of phosphate (Table 1). Differences in the phosphate binding affinities between mutants with neutral residues could be attributed to differences in polarity, H-bonding ability, and bulkiness of the side chains of studied neutral residues. In general, mutation of the negatively charged D94 residue to positively charged or neutral residues and the associated changes in phosphate binding affinity clearly showed the importance of the aspartate (D) residue and its charge at this particular position in OprP. In addition to charge, the bulkiness of the side chain might also have contributed in determining the binding affinity. The D94 mutants did not lead to major changes in single channel KCl conductance (G), in contrast to R133 mutants[21] (Table 1).

Furthermore, we also carried out zero current measurements to investigate changes in the ion selectivity of the D94 mutants compared with WT OprP. As a general trend, we observed that all D94 mutants retained anion selectivity (Table 2). Although decreases in the anion selectivity appear to have occurred for some D94 mutants compared with that for the WT channel, the selectivity of the mutant channels was in all cases close to the Nernst-limit, which made it difficult to quantify possible changes. The decrease in the anion selectivity for some of the

dx.doi.org/10.1021/cb500399j | ACS Chem. Biol. 2015, 10, 441–451

Table 2. Zero-Current Measurements to Study the Ion Selectivity of OprP and the D94 Mutants[a]

	permeability ratios, P_a/P_c (V_m [mV])				
electrolyte	D94	D94K	D94R	D94N	D94A
KCl	>70[17]	25 (−37.3 ± 1.3)	10 (−31.4 ± 2.5)	94 (−39.3 ± 0.2)	45 (−38.0 ± 0.9)

[a]The experiments were carried out for five-fold KCl gradients (0.1 M KCl versus 0.5 M KCl). The ratio of anion to cation permeability, (P_a/P_c) was calculated using the Goldman−Hodgkin−Katz equation[24] from at least three individual experiments. The zero-current membrane potential, V_m, is defined as the difference between the potential at the dilute side and that at the concentrated side of salt solutions. The selectivity for wild-type OprP (D94) was repeated recently and resulted in similar values as measured previously.[18,19]

mutants might be attributed to a stronger binding of Cl^- ions to the mutant proteins, which may lead to the slower concentration gradient-dependent permeation of Cl^- ions in the mutant channels compared with WT. Presumably, a stronger binding of Cl^- could be due to the absence of the electrostatically repellent negatively charged residue D94 in the central binding site in mutant channels.

To further probe and understand the importance of the D94 residue of OprP, we carried out free-energy molecular dynamics (MD) simulations to understand the energetics of phosphate, chloride, and potassium ion permeation through D94K mutant channels. As discussed above, a charge inversion mutation, D94K, resulted in strongest binding of the phosphate ion to the channel as observed in electrophysiological measurements. This mutant, in which the negatively charged residue D94 was mutated into a positive one, provided the opportunity to probe the role of negatively charged residues in the anion binding site for anion-selective channels when compared with the WT channel. Hence we calculated one-dimensional potential of mean force (PMF) profiles for the transport of different ions through the D94K mutant (Figure 2). PMF calculations include, in addition to electrostatic interactions, vdW interactions and entropic contributions that determine the overall interaction energies between the permeating ions and the channel. To facilitate comparisons, PMF profiles from our previous studies with the WT[17] and the R133E[21] channels are also shown. In addition, the PMF profile for phosphate transport through the D94R mutant was calculated to understand possible molecular factors underlying the stronger binding of phosphate in the D94K mutant compared with the D94R mutant even though both lysine (K) and arginine (R) are positively charged residues.

The PMF profile for the transport of $H_2PO_4^-$ through the D94K channel revealed two energetically favorable and very deep central binding sites with well depths as great as 16 kcal/mol (Figure 2a). The WT OprP channel included two similar central phosphate binding sites but with a well depth of only 8 kcal/mol (Figure 2a). Such a large increase in binding energy from WT OprP to the D94K mutant indicated a very strong binding of the phosphate within the mutant channel. This was well supported by the 30-fold increase in the phosphate binding affinity for the D94K mutant compared with WT in the electrophysiological experiments (Table 1).

The other mutation of the negatively charged D94 residue to the positively charged arginine (D94R) also showed an increase in binding affinity of phosphate in electrophysiological experiments. However, the binding to the D94R mutant was not as strong as that observed for the D94K mutant (Table 1). The PMF profile reinforced the experimental findings as phosphate experienced a well-depth of approximately 11 kcal/mol in the D94R mutant compared with the well-depth of 16 kcal/mol in the D94K mutant (Figure 2a). Figure 3 shows a molecular analysis revealing that the bulky side chain of the

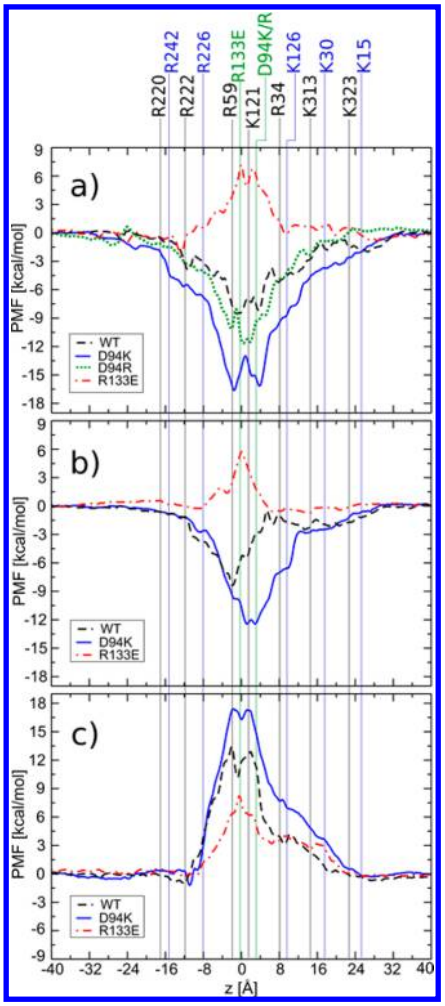

Figure 2. PMF profiles for the permeation of (a) $H_2PO_4^-$ through the D94K and D94R mutants of OprP and PMF profiles for the permeation of (b) Cl^- and (c) K^+ ions through the OprP mutant D94K. Data concerning the PMFs for the WT and R133E mutant channels are shown for comparison (see refs 17 and 21). Important residues of OprP along the ion permeation pathway are mapped onto the PMF profiles with respect to their positions along the z axis.

arginine residue in the D94R mutant acquired a different conformation upon entry of phosphate ions into the central binding region and consequently the arginine almost blocked the channel. In contrast, the lysine residue in the D94K mutant did not undergo any noticeable conformational changes upon the entry of phosphate into the central binding region and in turn did not block the channel (Figure 3). This different behavior of lysine and arginine in OprP mutants led to the observed changes in the PMF profiles and stronger binding of phosphate in the D94K mutant compared with the D94R mutant. In addition changes between the D94K and D94R

dx.doi.org/10.1021/cb500399j | ACS Chem. Biol. 2015, 10, 441−451

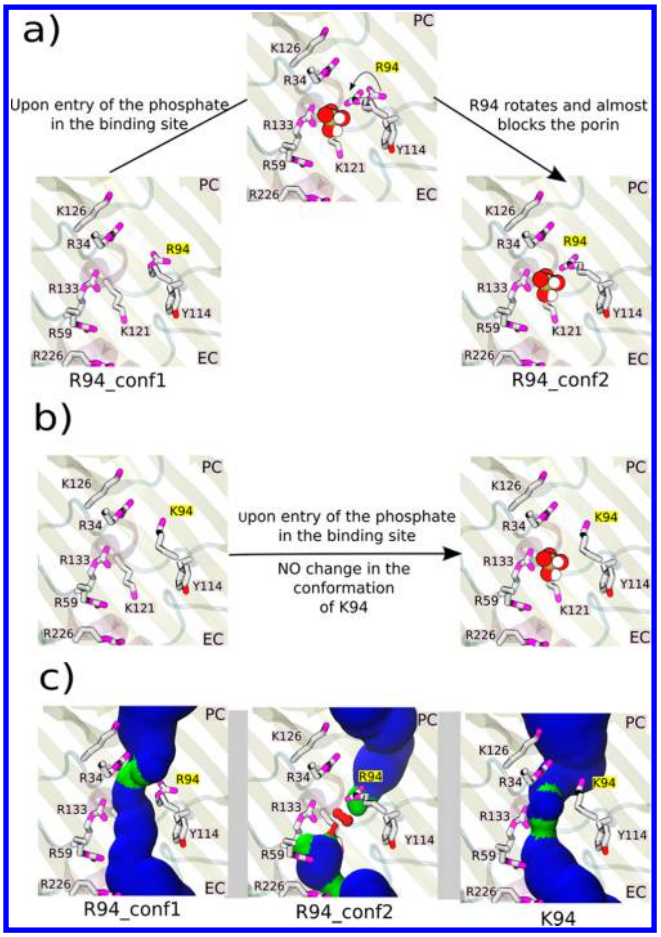

Figure 3. (a) Change in the conformation of the side chain of the R94 residue in the D94R mutant upon the entry of the phosphate in the binding site, leading to the R side chain almost blocking the porin. EC and PC represent the extracellular and periplasmic side of the channel, respectively. (b) Side chain of the K94 residue in the D94K mutant did not result in any observed conformational change upon the entry of phosphate in the binding site. (c) Approximate relative radii of D94R mutants (R94_conf1, R94_conf2) and D94K mutant are presented by a solid surface presentation and color coded according to the radius (blue, radius >2 Å; green, radius between 1 and 2 Å; red, radius <1 Å). Radii were calculated using the HOLE program.

mutants in the root-mean-square fluctuation (RMSF) values in simulations were observed, particularly for the residues of loop L3 (see Supporting Information, Figure S4). Loop L3 spans the entire central region of OprP (from −14 to 14 Å). Therefore, the observed changes between the PMF profiles of the D94K and D94R mutants can also be attributed to the difference in the dynamics of loop L3 in both mutants.

A large increase in phosphate binding affinity of the D94K mutant compared with WT could be compared with observations for the previously studied R133E mutant where a large decrease in phosphate binding affinity, approximately 40-fold, was observed both in experiments and in simulations.[21] The PMF profiles (Figure 2) together with the experimental observations demonstrated a role for the negative charge belonging to the D94 residue in regulating the binding affinity of phosphate to OprP. The D94 residue in OprP, despite its negative charge, maintained energetically favorable phosphate binding sites in the central region of the channel and at the same time prevented excessively strong binding of phosphate that would oppose phosphate flux through the channel. The biological importance of achieving, in this way, an appropriate binding affinity for the phosphate ion of OprP and other possible implications of the negative charge in the binding site of OprP are discussed below (see the Discussion section).

The PMF profiles for another anion, Cl^-, also revealed the stronger binding of chloride in the D94K channel compared with the WT pore (Figure 2b). The energetic depth of the binding site increased from 8 kcal/mol for the WT channel to 13 kcal/mol for the D94K mutant. This further confirmed the role of the D94 residue in regulating the appropriate binding affinity of anions in OprP. Furthermore, a decrease in the anion-to-cation permeability ratio, P_a/P_c, for the KCl electrolyte solution for D94K compared with WT (Table 2) might have resulted from slower permeation of Cl^- ions through the mutant channel, due to the stronger binding of anions to the mutant, as suggested by the PMF profiles (Figure 2b). K^+ ion transport through the D94K mutant demonstrated an increase in a barrier height compared with that in the WT channel (Figure 2c).

Such large changes in the PMF profiles and in turn the associated binding affinities for the permeating phosphate in response to point mutants of OprP are intriguing. To further understand them, we calculated electrostatic potential maps for

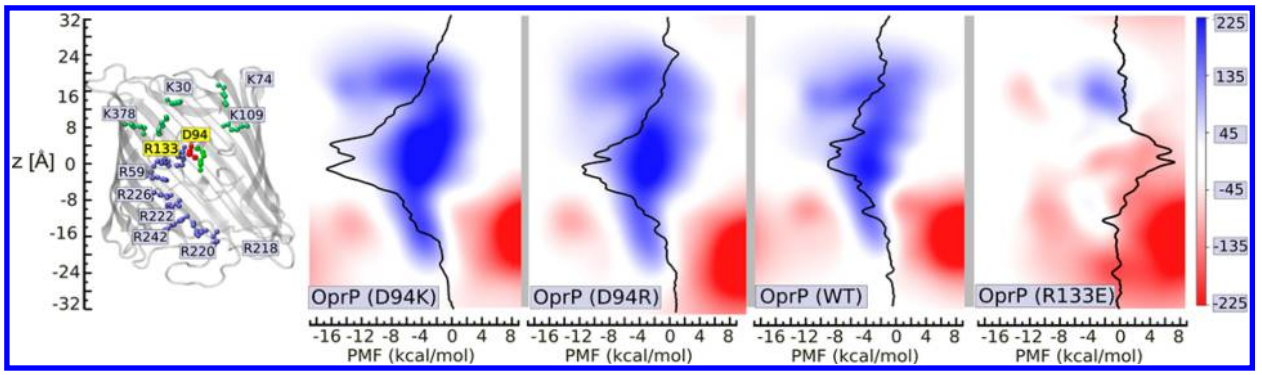

Figure 4. Electrostatic potential maps for the WT OprP and mutants D94K, D94R, and R133E. The OprP channel together with important residues were mapped along the electrostatic potential maps to enable identification of possible residues that were responsible for particular features of the potential maps. In addition, PMF profiles for the $H_2PO_4^-$ ion permeation through the WT and mutant channels were mapped onto the respective electrostatic potential maps indicating a correlation between the energetics of the $H_2PO_4^-$ transport and the electrostatic potential profiles. The potential maps are in the y−z plane at an x position corresponding to the middle of the one of the three pores and were generated using the PMEPlot plug-in for VMD.[25,26]

dx.doi.org/10.1021/cb500399j | ACS Chem. Biol. 2015, 10, 441−451

the WT channel and mutant channels of OprP. Potential maps were calculated using the PMEPlot plugin of VMD[25,26] and averaged over the equilibrium simulations of 25 ns length. As shown in Figure 4, the electrostatic potential maps showed large changes with respect to point mutations particularly in the central region of the pore. Compared with WT OprP, the D94K mutant displayed a very strong electropositive region at the center of the channel (Figure 4), which likely explains the very strong binding of the negatively charged phosphate or chloride in the D94K mutant. The D94R mutant also had a strong electropositive region at the center of the channel, which was, within statistical uncertainties, rather similar to the D94K mutant. Conversely, the R133E mutant did not show such an electropositive region at the center of the channel in the potential map (Figure 4). This observation rationalized the PMF profile for phosphate ions, which was void of any energetically favorable affinity region for this particular mutant. Furthermore, we mapped the respective PMF profiles for $H_2PO_4^-$ permeation through each of the channels to enable comparisons (Figure 4). A clear correlation between the electropositive and electronegative features of the electrostatic potential maps and the PMF profiles was visible. It was also interesting to observe such "global" effects on the electrostatic potential maps of OprP in response to single point mutants, which was due to the long-range nature of the electrostatic interactions.

In further analyses, we calculated the electrostatic interaction energies between the permeating ions and the channel at different regions of the pore (Figure 5). For this purpose, the pore was divided into 1 Å bins and the interaction energies were calculated with a cutoff distance of 12 Å using the NAMDenergy plugin. Compared with the WT, $H_2PO_4^-$ ions experienced more favorable electrostatic interaction energies within the central region of the pore for the D94K and D94R mutants (Figure 5a). This finding was in accordance with the PMF profiles (Figure 2a) and electrostatic potential maps of the WT and the D94K channels (Figure 4), as described above. Hence the stronger binding of $H_2PO_4^-$ in the D94K mutant compared with the D94R mutant was not due to electrostatic effects but rather to the different side chain conformation of the arginine residue in the D94R mutant compared with the lysine of D94K as discussed previously. Similarly, Cl^- ions showed more favorable electrostatic interaction energies in the central region of the pore for the D94K mutant compared with the WT channel (Figure 5b). In contrast, due to the very strong electropositive potential of the D94K mutant, the K^+ ions were subject to very unfavorable electrostatic interaction energies for this particular mutant (Figure 5c). This phenomena was also reflected in the PMF profile with an energetic barrier that was as high as +17 kcal/mol for the permeation of K^+ ions through the D94K mutant.

The above studies focused on the electrostatic component of the energy between the permeating ion and the channel, which indeed largely determined the stronger binding of phosphate in the D94K channel compared with WT. However, water molecules played an important role in regulating the interactions between the permeating ions and the channel. To interact with the channel, the permeating ions had to be stripped of at least some of the water molecules belonging to the hydration shell, particularly in the narrowest central region of the pore where the channel radius is smaller than the hydrodynamic radius of the permeating ions. Ion selectivity and ion transport properties of channels are believed to be

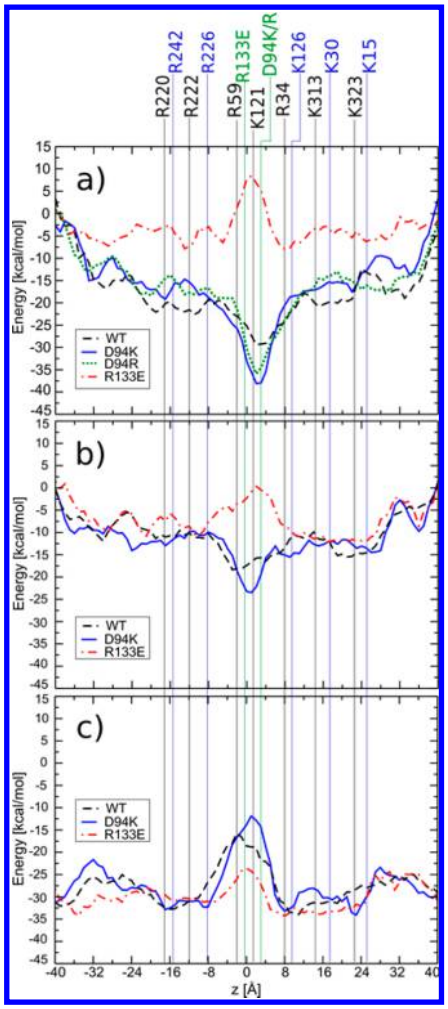

Figure 5. Electrostatic interaction energy for (a) $H_2PO_4^-$ transport through the D94K and D94R mutants of OprP, and for (b) Cl^- and (c) K^+ ions passing through the OprP mutant D94K. Data for the electrostatic energy for the WT and R133E mutant channels are shown for comparison (see refs 17 and 21). All energy values denote relative interaction energies assuming zero interaction energies in the bulk phase.

determined by the interactions and interplay between permeating ions, surrounding water molecules and the channel. For example, we already showed the importance of the residue R133 of OprP in governing the phosphate binding affinity through its ability to dehydrate the permeating ion in conjunction with the network of other residues in OprP.[21] Particularly for anion selective channels, the hydration energy of the permeating ions was reported to be responsible for the rate-limiting step in determining ion transport processes.[27−29]

To understand the effect of the hydration shell, we carried out a coordination number analysis for permeating ions in different regions of the pore for the D94K mutant. A detailed procedure for calculating the coordination number is provided elsewhere.[17,21] As the permeating ions move inside the channel, a portion of the water molecules would be removed from the respective hydration shell, which would be compensated by protein contacts. As shown in Figure 6a, the $H_2PO_4^-$ ions stripped off eight water molecules in the central region of the pore to enable passage through the positively charged D94K and D94R mutants. Compared with this, $H_2PO_4^-$ ions had to strip off seven and four water molecules while permeating

dx.doi.org/10.1021/cb500399j | ACS Chem. Biol. 2015, 10, 441−451

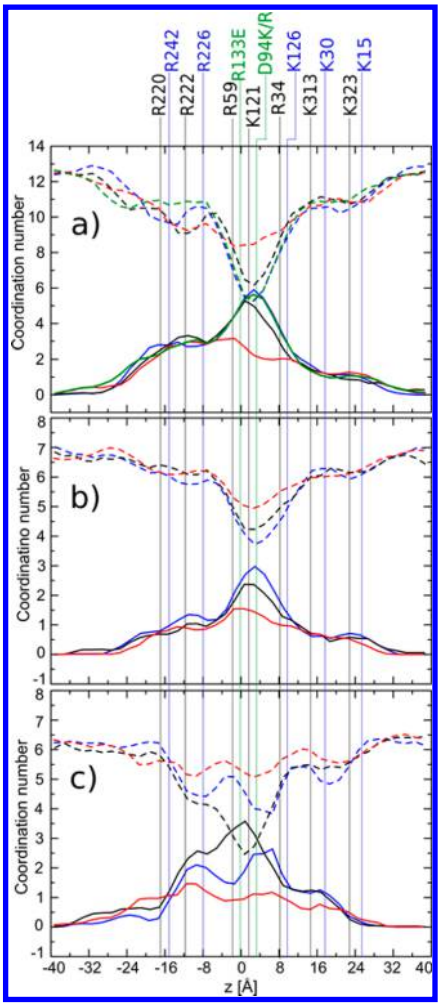

Figure 6. Coordination numbers for the water (dashed line) and protein (solid line) contacts for the transport of the ions (a) $H_2PO_4^-$, (b) Cl^-, and (c) K^+ through the OprP mutant channels D94K (blue), D94R (green), WT (black), and R133E (red). Data for the WT and R133E mutant channels are shown for comparison (refs 17 and 21).

through the WT and the R133E channel, respectively. Removal of more water molecules from the hydration shell during passage through a channel, for example, the D94K and D94R channels, results from a stronger affinity of phosphate for that particular channel (Figure 6a). Conversely, stripping off less water molecules, for example, in the R133E channel, results from a weaker binding of the phosphate in the respective channel. For the other studied anion, Cl^-, a similar correlation between the removal of water molecules from the hydration shell and binding affinity was observed (Figure 6b).

DISCUSSION

With the help of bilayer electrophysiological measurements, we revealed how and why phosphate binding affinity varied when the D94 residue was mutated to other amino acids. Mutation of the negatively charged D94 residue to the tested positively charged or neutral residue led to an increased binding affinity for phosphate. Of particular interest were the charge inversion mutations for D94 and in particular D94K for which an approximately 30-fold increase in the binding affinity of the phosphate ion was observed. Free-energy MD simulations provided a possible molecular picture explaining such strong affinities of the D94K mutant for phosphate. The difference in the binding affinity of phosphate between the D94K and D94R mutants could be mainly explained by the different side chain conformations of lysine and arginine in the presence of phosphate in the binding site (Figure 3). These mutants of D94 revealed that the presence of a negatively charged D94 residue in the affinity site reduced the very strong binding of the phosphate in WT OprP. The biological significance of achieving an appropriate binding affinity of phosphate to OprP and possible importance of the aspartate residue in the affinity site of OprP is further discussed below.

In nature, channels and porins are designed to allow the permeation of ions and substrates through otherwise impermeable membranes. On the one hand, binding of the permeating ions or substrates inside the channel helps to ensure substrate specificity and selectivity for channels, which is essential to their functioning. In particular OprP is induced in the bacterium *Pseudomonas aeruginosa* under phosphate-limiting conditions, with growth-limiting phosphate concentrations that are required to induce OprP being as low as 0.15 mM phosphate.[6] Thus, the presence of defined binding sites in the channel with affinity for phosphate enhances the efficiency of phosphate uptake from dilute environments. On the other hand, very strong binding of the phosphate inside the channel would lead to inefficient and slow permeation because the transport at higher phosphate concentration would be limited by the off-rate constant of phosphate binding to the binding site in a one-site two-barrier model. Hence, the appropriate binding affinity for phosphate is essentially a trade-off between tight binding and permeation efficiency, which is necessary for the appropriate functioning of the OprP channel.

One additional and important dimension to the significance of achieving the appropriate binding affinity for phosphate in OprP is the role of the periplasmic phosphate-binding protein (PBP) as a part of the phosphate transport system (PTS) in *P. aeruginosa*.[7] Since *in vivo* the phosphate movement must be unidirectional, from the extracellular to the periplasmic side, in order to meet the cellular nutritional requirements of the bacterium, an additional high-affinity component in the form of a periplasmic PBP facilitates unidirectional uptake across the outer membrane because it prevents free phosphate from accumulating in the periplasm. The presence and role of the periplasmic PBP in mediating high-affinity phosphate transport was confirmed by mutagenesis in *P. aeruginosa*. In the wild-type, which contains PBP and OprP, two kinetically distinct systems were observed for phosphate uptake, one with high-affinity and the other low-affinity.[30,31] In contrast, only a single low-affinity transport system was observed in the mutant lacking the binding protein, suggesting the role of the binding protein in inducible high-affinity phosphate-uptake system of *P. aeruginosa*. The role of the similar collaborations between an outer membrane specific channel (LamB) and a periplasmic binding protein was previously established as part of the maltose/maltodextrin uptake system of *E. coli*.[32,33] *In vivo*, phosphate binds first to medium affinity sites within OprP and subsequently binds to the higher affinity periplasmic phosphate-binding protein to enable passage of phosphate across the outer membrane. Of critical importance is an "appropriate" interaction strength of the phosphate ions within the OprP channel to allow phosphate ions to be taken up from the dilute extracellular environment and then to allow these ions to dissociate from the channel to enable their association with the phosphate-binding protein. The presence of the negatively charged D94 in OprP thus is biologically important

dx.doi.org/10.1021/cb500399j | *ACS Chem. Biol.* 2015, 10, 441−451

Table 3. Mutants Designed To Investigate the Contribution of the Amino Acid D94 in Ion Selectivity and Phosphate Substrate Specificity[a]

OprP	codon	5′−3′ primer	amino acid side chain
D94 (WT)	GAC	not mutated	$-CH_2-COO^-$
D94K	AAG	GCGCCGGCTACTTT**AAG**GAAGCTTCGGTCAC	$-CH_2-CH_2-CH_2-CH_2-NH_3^+$
D94R	CGC	GCGCCGGCTACTTT**CGC**GAAGCTTCGGTCAC	$-CH_2-CH_2-CH_2-NH-C(NH_2^+)-NH$
D94N	AAC	GCGCCGGCTACTTT**AAC**GAAGCTTCGGTCAC	$-CH_2-CO-NH_2$
D94Q	CAG	GCGCCGGCTACTTT**CAG**GAAGCTTCGGTCAC	$-CH_2-CH_2-CO-NH_2$
D94A	GCC	GCGCCGGCTACTTT**GCC**GAAGCTTCGGTCAC	$-CH_3$

[a]Mutants are named by the mutated residue (D94) followed by the new residue (e.g., K as in D94K), according to the one letter amino acid code. The codons of the wild-type and mutants are indicated in addition to the forward primers used to mutate them. The side chains of the various amino acids and any charges at neutral pH are also displayed.

for achieving such an appropriate binding affinity for the phosphate.

One further important aspect of the phosphate selectivity of OprP is to enable discrimination of phosphate from a very similar, tetrahedral-shaped oxyanion, that is, sulfate. At the physiological pH of around 7, phosphate can exists in monobasic ($H_2PO_4^-$) or dibasic (HPO_4^{2-}) form, while sulfate stays in its fully ionized dibasic (SO_4^{2-}) form in this pH regime. In nature, a precedent for molecular recognition that allows the discrimination between phosphate and sulfate can be realized based on the examples of the phosphate-binding protein (PBP) and the sulfate-binding protein (SBP). The ability of the PBP and SBP to exquisitely discriminate between phosphate and sulfate has been attributed to the presence of an aspartate residue in the binding site of PBP and the corresponding absence of an aspartate residue in the binding site of SBP.[34−37] Phosphate, in its physiologically available protonation states, can act as a H-bond donor and can specifically interact with the H-bond acceptor carboxylate group of the aspartate side chain. However, sulfate, in not possessing a H-bond donor, cannot form such specific interactions with the aspartate residue and is thus subject to charge repulsion. OprP, being a phosphate-selective porin, thus can achieve excellent specificity for phosphate over sulfate due to the presence of the D94 residue in the binding site.

In addition to the above, by forming salt bridges with R34, R59, and R60 (see Figure 1a), the D94 residue in OprP might also help to stabilize the protonation states and in turn the positive charges of this cluster of three consecutive arginine residues in the narrowest region of the pore. The positive charges of these arginine residues are very important for maintaining the phosphate binding affinity of OprP. It was reported for the *E. coli* OmpF and PhoE channels that the close proximity of three adjoining arginine side chains might confer unusual ionization behavior leading to deprotonated forms of these arginines.[38] Conversely, for the anion-selective porin Omp32 from *Delftia acidovorans*, the protonation states and positive charges of arginines from the arginine cluster were indicated to be stabilized by the formation of salt-bridges with a glutamate (E58) residue.[39]

In biology, the functional importance of an amino acid can usually be justified based on its evolutionary conservation. The D94 residue of OprP from *P. aeruginosa* is evolutionarily conserved between different OprP orthologs in *Pseudomonas* species (Supporting Information, Figure S5). However, a similar conservation of a negatively charged residue in other anion-selective porins would suggest a general design principle, based on the above-described considerations, involving negatively charged residues in the anion binding sites of anion-selective porins. Among the few reported strongly anion-selective porins, the crystal structure of Omp32 porin from *Delftia acidovorans* is also available. The Omp32 porin is a strongly anion-selective porin[40] and has a negatively charged residue, E58, in its anion binding site, as also demonstrated by the corresponding PMF profile.[41] *Delftia acidovorans* belongs to the group of β-proteobacteria,[42] and the sequence of Omp32 is similar to that of other reported anion-selective porins from the same group, namely, the porins from *Bordetella pertussis*,[43] *Neisseria gonorrheae*,[44] *Neisseria meningitidis*,[45] and *Acidovorax delafieldii*.[46] Most important is the conservation of the residue E58 in the anion-selective porins of all of these bacteria from the β-proteobacteria group, thus supporting the importance of a negatively charged residue in an anion binding site (Supporting Information, Figure S6).

In conclusion, we have shown the importance of residue D94 of OprP in conferring an appropriate binding affinity of phosphate toward OprP. The mutation of the negatively charged residue at position 94 to positively charged or neutral residues, particularly lysine (K), led to a stronger binding for phosphate in OprP, as observed in both electrophysiological bilayer measurements and free-energy MD simulations. The stronger binding of phosphate in the D94K mutant compared with the D94R mutant was explained by the different side chain conformations of these two positively charged residues in the presence of phosphate in the binding site. The computer simulations presented here provided molecular insights regarding the importance of D94 in OprP and complemented the electrophysiological experiments. In future such simulations on porins systems could be done in their natural membrane environment, that is, an asymmetric membrane that includes lipopolysaccharide (LPS) molecules.[47] It would be interesting to investigate how some of the loops of porins interact with the LPS membrane. The use of polarizable force fields[48,49] and constant pH simulations[50] that allow protonation state to be defined based on the local environment could further improve the accuracy of the molecular dynamics simulations.

Our data favor the possible relevance of the D94 residue in the wild-type channel in attaining an appropriate binding affinity for phosphate toward OprP to achieve an efficient and unidirectional transport of phosphate across the outer membrane of *P. aeruginosa*. Other than that, the importance of the D94 residue in conferring, to OprP, selectivity for phosphate over sulfate, and the possible role of D94 in stabilizing the protonation states and charges of arginine clusters were also implicated. The presence of a similar negatively charged residue in the anion-selective porins of the β-proteobacteria group of bacteria further reinforces the broader importance of negatively charged residues in anion

dx.doi.org/10.1021/cb500399j | ACS Chem. Biol. 2015, 10, 441−451

binding sites of anion-selective porins. Molecular insights presented here can be useful in designing a "model" anion binding site for biomimetic anion-selective porins and channels.

METHODS

Bacterial Strains and Growth Conditions. *Escherichia coli* strain DH5α (Invitrogen, CA, United States) was utilized to host the plasmid containing the OprP gene pAS27[51] and several plasmids derived from it containing single amino acid mutations of this gene. *E. coli* CE1248,[52] an OmpC/OmpF/PhoE deficient strain, was employed to express the OprP porin and its mutants.[21]

Site-Directed Mutagenesis and Sequencing of OprP Mutants. The pAS27 plasmid was mutated and amplified using the Quick-Change mutagenesis kit (Stratagene, USA) following the standard protocol provided by the manufacturer.[21] Table 3 lists the primers utilized to perform the single mutations. The primers were synthesized by AlphaDNA (Montreal, Canada). Table 3 also lists the mutagenic codons consisting of mismatches that corresponded to the substitution mutation in the encoded amino acid sequence of OprP. The OprP sequence together with the sequences of the generated mutants were corroborated by the Nucleic Acid Protein Service Unit (University of British Columbia, Vancouver, Canada).

Protein Extraction and Purification. The different OprP D94 mutant proteins were extracted from *E. coli* CE1248 pellets as described previously.[21] Purification of the OprP native and D94 mutant proteins was achieved using a MonoQ column (Pharmacia, United States) coupled to a FPLC system using a NaCl gradient as described elsewhere.[21] OprP and its mutant proteins eluted at a salt concentration of 250−300 mM NaCl.

Sodium Dodecyl Sulfate-Polyacrylamide Gel Electrophoresis (SDS-Page) and Western Immunoblotting (WB). To confirm the expression and purification of the OprP mutants, whole cell lysates of *E. coli* CE1248 or the FPLC fractions were loaded onto a 12% SDS polyacrylamide gel and electrophoresed. The gels were stained with Coomassie blue or transferred to poly(vinylidene fluoride) (PVDF) membranes and incubated with monomer-specific anti-OprP rabbit serum as previously described.[51] *E. coli* CE1248 harboring pAS27 and *E. coli* CE1248 harboring the vector plasmid pTZ19U (Pharmacia, USA) were used as positive and negative controls, respectively.[21]

Black Lipid Bilayer: Single Channel Conductance, Zero Current Measurements, and Phosphate Titration. The black lipid planar bilayer assay using membranes made up of the 1% 1,2-diphytanoylphosphatidylcholine (DiPhPC) in *n*-decane has been described elsewhere.[53] Measurements to investigate inhibition of chloride conductance mediated due to phosphate binding to the binding sites were performed for OprP D94 mutants by titrating potassium phosphate, pH 6, into one chamber of the planar bilayer apparatus in which a DiPhPC membrane containing OprP or one of its mutants was reconstituted.[21,23,54] The half saturation constant for decrease in chloride conductance through OprP and its mutants, due to phosphate binding, was calculated utilizing the Langmuir isotherm or the Michaelis−Menten equation.[21,55] Previously it has been shown experimentally that phosphate binds more strongly to OprP in its monobasic form than in its dibasic form.[6] In that study, electrophysiological measurements were done at different pH values where phosphate can exist predominantly as either monobasic (pH 4 and 6) or dibasic (pH 8) forms and phosphate has a stronger binding to OprP in its monobasic form. Therefore, pH 6 was chosen for the present study to have a unique and well-defined protonation state of the phosphate ions. Zero current potential measurements to study ion selectivity were performed as described previously.[21,24,53]

Molecular Dynamics Simulations. The OprP trimer (PDB code 2O4V)[20] was embedded into a bilayer consisting of palmitoyloleoyl-glycero-phosphatidyl ethanolamine (POPE) lipids.[25] TIP3P water molecules were used to solvate the protein embedded bilayer system. Moreover, the D94 residues in each of the monomers were mutated to lysine (K) and arginine (R) to generate the D94K and D94R mutants, respectively. Subsequently the ion under the investigation, that is, phosphate, chloride, or potassium, was placed at the mouth of the one of the monomers on the extracellular side of the mutant protein.[17,21] The monobasic form of the phosphate ion, $H_2PO_4^-$, was considered in agreement with our previous studies.[17,21] Phosphate is predominantly in its monobasic form at pH 6 at which experimental measurements are done. The simulations were carried out in the NPT ensemble at a temperature of 310 K and a pressure of 1 atm utilizing the NAMD 2.9 program.[56] The CHARMM27 force field[57] together with the additional force field parameters for $H_2PO_4^-$[58] was employed. The bonded interactions were calculated every 1 fs, while the short-range nonbonded and the long-range electrostatic interactions were calculated every 2 and 4 fs, respectively. In order to determine the effective free energy profiles for the permeation of various ions through OprP mutants, the adaptive biasing force (ABF) method[59−61] as available in the *collective variable* module of the NAMD 2.9 program was utilized. Further details about the system setup, simulation parameters, and free-energy calculations can be found elsewhere.[21]

ASSOCIATED CONTENT

Supporting Information

Further experimental details, sequence alignments, and other analyses. This material is available free of charge via the Internet at http://pubs.acs.org.

AUTHOR INFORMATION

Corresponding Author

*E-mail: u.kleinekathoefer@jacobs-university.de.

Author Contributions

§N.M. and I.B.-U. contributed equally.

Notes

The authors declare no competing financial interest.

ACKNOWLEDGMENTS

The authors thank Q.-T. Tran for her contribution at the early stage of this study. The research leading to these results was conducted as part of the Translocation consortium (www.translocation.eu) and has received support from the Innovative Medicines Joint Undertaking under Grant Agreement No. 115525, resources that are composed of financial contribution from the European Union's seventh framework programme (FP7/2007-2013) and EFPIA companies in kind contribution. This work was also supported by Grants KL 1299/6-1 and BE 865/16-1 of the Deutsche Forschungsgemeinschaft (DFG), and a Canadian Institutes for Health Research grant to R.E.W.H. who also has a Canada Research Chair in Health and Genomics.

REFERENCES

(1) Kuriyan, J., Konforti, B., and Wemmer, D. (2013) *The Molecules of Life: Physical and Chemical Principles*, Garland Science, Taylor & Francis Group.

(2) Fischer, E. (1894) Einfluss der configuration auf die wirkung der enzyme. *Ber. Dtsch. Chem. Ges. 27*, 2985−2993.

(3) Pauling, L., and Delbrück, M. (1940) The nature of the intermolecular forces operative in biological processes. *Science 92*, 77−79.

(4) Koshland, D., Jr (1958) Application of a theory of enzyme specificity to protein synthesis. *Proc. Natl. Acad. Sci. U. S. A. 44*, 98.

(5) Hille, B. (2001) *Ion Channels of Excitable Membranes*, 3rd ed., Sinauer, Sunderland, MA.

(6) Benz, R., Egli, C., and Hancock, R. E. W. (1993) Anion transport through the phosphate-specific OprP-channel of the *Pseudomonas aeruginosa* outer membrane: Effects of phosphate, di-and tribasic anions and of negatively-charged lipids. *Biochim. Biophys. Acta, Biomembr. 1149*, 224−230.

(7) Worobec, E. A., Siehnel, R. J., Gladman, P., and Hancock, R. E. W. (1988) Gene cloning and expression of the *Pseudomonas aeruginosa* periplasmic phosphate-binding protein. *FEMS Microbiol. Lett. 52*, 235–238.
(8) Varma, S., and Rempe, S. (2007) Tuning ion coordination architectures to enable selective partitioning. *Biophys. J. 93*, 1093–1099.
(9) Noskov, S., Bernéche, S., and Roux, B. (2004) Control of ion selectivity in potassium channels by electrostatic and dynamic properties of carbonyl ligands. *Nature 431*, 830–834.
(10) Fowler, P. W., Tai, K., and Sansom, M. S. (2008) The selectivity of K+ ion channels: Testing the hypotheses. *Biophys. J. 95*, 5062–5072.
(11) Noskov, S., and Roux, B. (2007) Importance of hydration and dynamics on the selectivity of the KcsA and NaK channels. *J. Gen. Physiol. 129*, 135–143.
(12) Cohen, J., and Schulten, K. (2004) Mechanism of anionic conduction across ClC. *Biophys. J. 86*, 836–845.
(13) Ivanov, I., Cheng, X., Steven, M., and McCammon, J. (2007) Barriers to ion translocation in cationic and anionic receptors from the Cys-loop family. *J. Am. Chem. Soc. 129*, 8217–8224.
(14) Hancock, R. E. W., Poole, K., and Benz, R. (1982) Outer membrane protein P of *Pseudomonas aeruginosa*: Regulation by phosphate deficiency and formation of small anion-specific channels in lipid bilayer membranes. *J. Bacteriol. 150*, 730–738.
(15) Benz, R., and Hancock, R. E. W. (1987) Mechanism of ion transport through the anion-selective channel of the *Pseudomonas aeruginosa* outer membrane. *J. Gen. Physiol. 89*, 275–295.
(16) Hancock, R. E. W., and Benz, R. (1986) Demonstration and chemical modification of a specific phosphate binding site in the phosphate-starvation-inducible outer membrane porin protein P of *Pseudomonas aeruginosa*. *Biochim. Biophys. Acta, Biomembr. 860*, 699–707.
(17) Modi, N., Benz, R., Hancock, R. E. W., and Kleinekathöfer, U. (2012) Modeling the ion selectivity of the phosphate specific channel OprP. *J. Phys. Chem. Lett. 3*, 3639–3645.
(18) Pongprayoon, P., Beckstein, O., Wee, C. L., and Sansom, M. S. (2009) Simulations of anion transport through OprP reveal the molecular basis for high affinity and selectivity for phosphate. *Proc. Natl. Acad. Sci. U. S. A. 106*, 21614–21618.
(19) Pongprayoon, P., Beckstein, O., and Sansom, M. S. P. (2012) Biomimetic design of a brush-like nanopore: Simulation studies. *J. Phys. Chem. B 116*, 462–468.
(20) Moraes, T., Bains, M., Hancock, R. E. W., and Strynadka, N. (2006) An arginine ladder in OprP mediates phosphate-specific transfer across the outer membrane. *Nat. Struct. Mol. Biol. 14*, 85–87.
(21) Modi, N., Bárcena-Uribarri, I., Bains, M., Benz, R., Hancock, R. E. W., and Kleinekathöfer, U. (2013) Role of the central arginine R133 towards the ion selectivity of the phosphate specific channel OprP: Effects of charge and solvation. *Biochemistry 52*, 5522–5532.
(22) Oliva, R., Calamita, G., Thornton, J. M., and Pellegrini Calace, M. (2010) Electrostatics of aquaporin and aquaglyceroporin channels correlates with their transport selectivity. *Proc. Natl. Acad. Sci. U. S. A. 107*, 4135–4140.
(23) Benz, R., Schmid, A., and Vos Scheperkeuter, G. H. (1987) Mechanism of sugar transport through the sugar-specific LamB channel of *Escherichia coli* outer membrane. *J. Membr. Biol. 100*, 21–29.
(24) Ludwig, O., De Pinto, V., Palmieri, F., and Benz, R. (1986) Pore formation by the mitochondrial porin of rat brain in lipid bilayer membranes. *Biochim. Biophys. Acta, Biomembr. 860*, 268.
(25) Humphrey, W. F., Dalke, A., and Schulten, K. (1996) VMD – Visual Molecular Dynamics. *J. Mol. Graphics 14*, 33–38.
(26) Aksimentiev, A., and Schulten, K. (2005) Imaging alpha-hemolysin with molecular dynamics: ionic conductance, osmotic permeability, and the electrostatic potential map. *Biophys. J. 88*, 3745–3761.
(27) Bormann, J., Hamill, O., and Sakmann, B. (1987) Mechanism of anion permeation through channels gated by glycine and gamma-aminobutyric acid in mouse cultured spinal neurones. *J. Physiol. 385*, 243–286.
(28) Verdon, B., Winpenny, J., Whitfield, K., Argent, B., and Gray, M. (1995) Volume-activated chloride currents in pancreatic duct cells. *J. Membr. Biol. 147*, 173–183.
(29) Linsdell, P., and Hanrahan, J. (1998) Adenosine triphosphate–dependent asymmetry of anion permeation in the cystic fibrosis transmembrane conductance regulator chloride channel. *J. Gen. Physiol. 111*, 601–614.
(30) Lacoste, A.-M., Cassaigne, A., and Neuzil, E. (1981) Transport of inorganic phosphate in *Pseudomonas aeruginosa*. *Curr. Microbiol. 6*, 115–120.
(31) Poole, K., and Hancock, R. E. W. (1984) Phosphate transport in *Pseudomonas aeruginosa*. *Eur. J. Biochem. 144*, 607–612.
(32) Bavoil, P., and Nikaido, H. (1981) Physical interaction between the phage lambda receptor protein and the carrier-immobilized maltose-binding protein of *Escherichia coli*. *J. Biol. Chem. 256*, 11385–11388.
(33) Ferenci, T., and Boos, W. (1980) The role of the *Escherichia coli* λ receptor in the transport of maltose and maltodextrins. *J. Supramol. Struct. 13*, 101–116.
(34) Pflugrath, J. W., and Quiocho, F. A. (1988) The 2 Å resolution structure of the sulfate-binding protein involved in active transport in *Salmonella typhimurium*. *J. Mol. Biol. 200*, 163–180.
(35) Luecke, H., and Quiocho, F. A. (1990) High specificity of a phosphate transport protein determined by hydrogen bonds. *Nature 347*, 402–406.
(36) Pflugrath, J., and Quiocho, F. (1985) Sulphate sequestered in the sulphate-binding protein of *Salmonella typhimurium* is bound solely by hydrogen bonds. *Nature 314*, 257–260.
(37) Quiocho, F. A. (1996) Atomic basis of the exquisite specificity of phosphate and sulfate transport receptors. *Kidney Int. 49*, 943–946.
(38) Karshikoff, A., Spassov, V., Cowan, S. W., Ladenstein, R., and Schirmer, T. (1994) Electrostatic properties of two porin channels from *Escherichia coli*. *J. Mol. Biol. 240*, 372–374.
(39) Zachariae, U., Koumanov, A., Engelhardt, H., and Karshikoff, A. (2002) Electrostatic properties of the anion selective porin Omp32 from *Delftia acidovorans* and of the arginine cluster of bacterial porins. *Protein Sci. 11*, 1309–1319.
(40) Mathes, A., and Engelhardt, H. (1998) Nonlinear and asymmetric open channel characteristics of an ion-selective porin in planar membranes. *Biophys. J. 75*, 1255–1262.
(41) Zachariae, U., Helms, V., and Engelhardt, H. (2003) Multistep mechanism of chloride translocation in a strongly anion-selective porin channel. *Biophys. J. 85*, 954–962.
(42) Nikaido, H. (2003) Molecular basis of bacterial outer membrane permeability revisited. *Microbiol. Mol. Biol. Rev. 67*, 593–656.
(43) Armstrong, S., Parr, T., Parker, C., and Hancock, R. E. W. (1986) *Bordetella pertussis* major outer membrane porin protein forms small, anion-selective channels in lipid bilayer membranes. *J. Bacteriol. 166*, 212–216.
(44) Mauro, A., Blake, M., and Labarca, P. (1988) Voltage gating of conductance in lipid bilayers induced by porin from outer membrane of *Neisseria gonorrhoeae*. *Proc. Natl. Acad. Sci. U. S. A. 85*, 1071–1075.
(45) Song, J., Minetti, C. A., Blake, M., and Colombini, M. (1998) Successful recovery of the normal electrophysiological properties of PorB (Class 3) porin from *Neisseria meningitidis* after expression in *Escherichia coli* and renaturation. *Biochim. Biophys. Acta, Biomembr. 1370*, 289–298.
(46) Brunen, M., and Engelhardt, H. (1993) Asymmetry of orientation and voltage gating of the *Acidovorax delafieldii* porin Omp34 in lipid bilayers. *Eur. J. Biochem. 212*, 129–135.
(47) Piggot, T. J., Holdbrook, D. A., and Khalid, S. (2013) Conformational dynamics and membrane interactions of the *E. coli* outer membrane protein FecA: A molecular dynamics simulation study. *Biochim. Biophys. Acta, Biomembr. 1828*, 284–293.
(48) Yu, H., Whitfield, T., Harder, E., Lamoureux, G., Vorobyov, I., Anisimov, V., MacKerell, A., Jr., and Roux, B. (2010) Simulating

monovalent and divalent ions in aqueous solution using a Drude polarizable force field. *J. Chem. Theory Comput. 6*, 774−786.
(49) Jiang, W., Hardy, D. J., Phillips, J. C., MacKerell, A. D., Schulten, K., and Roux, B. (2011) High-performance scalable molecular dynamics simulations of a polarizable force field based on classical drude oscillators in NAMD. *J. Phys. Chem. Lett. 2*, 87−92.
(50) Donnini, S., Tegeler, F., Groenhof, G., and Grubmüller, H. (2011) Constant pH molecular dynamics in explicit solvent with λ-dynamics. *J. Chem. Theory Comput. 7*, 1962−1978.
(51) Sukhan, A., and Hancock, R. E. W. (1995) Insertion mutagenesis of the *Pseudomonas aeruginosa* phosphate-specific porin OprP. *J. Bacteriol. 177*, 4914−4920.
(52) Bauer, K., Struyve, M., Bosch, D., Benz, R., and Tommassen, J. (1989) One single lysine residue is responsible for the special interaction between polyphosphate and the outer membrane porin PhoE of *Escherichia coli*. *J. Biol. Chem. 264*, 16393−16398.
(53) Benz, R., Janko, K., and Lauger, P. (1979) Ionic selectivity of pores formed by the matrix protein (porin) of *Escherichia coli*. *Biochim. Biophys. Acta, Biomembr. 551*, 238−247.
(54) Benz, R., Schmid, A., Nakae, T., and Vos Scheperkeuter, G. (1986) Pore formation by LamB of *Escherichia coli* in lipid bilayer membranes. *J. Bacteriol. 165*, 978−986.
(55) Thein, M., Bonde, M., Bunikis, I., Denker, K., Sickmann, A., Bergström, S., and Benz, R. (2012) DipA, a pore-forming protein in the outer membrane of lyme disease spirochetes exhibits specificity for the permeation of dicarboxylates. *PLoS One 7*, No. e36523.
(56) Phillips, J. C., Braun, R., Wang, W., Gumbart, J., Tajkhorshid, E., Villa, E., Chipot, C., Skeel, R. D., Kale, L., and Schulten, K. (2005) Scalable molecular dynamics with NAMD. *J. Comput. Chem. 26*, 1781−1802.
(57) MacKerell, A. D., Jr., Bashford, D., Bellot, M., Dunbrack, R. L., Jr., Evanseck, J. D., Field, M. J., Fischer, S., Gao, J., Guo, H., Ha, S., Joseph-McCarthy, D., Kuchnir, L., Kuczera, K., Lau, F. T. K., Mattos, C., Michnick, S., Ngo, T., Nguyen, D. T., Prodhom, B., Reiher, W. E., III, Roux, B., Schlenkrich, M., Smith, J. C., Stote, R., Straub, J., Watanabe, M., Wiórkiewicz-Kuczera, J., Yin, D., and Karplus, M. (1998) All-atom empirical potential for molecular modeling and dynamics studies of proteins. *J. Phys. Chem. B 102*, 3586−3616.
(58) Kleinekathöfer, U., Isralewitz, B., Dittrich, M., and Schulten, K. (2011) Domain motion of individual F1-ATPase β-subunits during unbiased molecular dynamics simulations. *J. Phys. Chem. A 115*, 7267−7274.
(59) Darve, E., and Pohorille, A. (2001) Calculating free energies using average force. *J. Chem. Phys. 115*, 9169−9183.
(60) Hénin, J., and Chipot, C. (2004) Overcoming free energy barriers using unconstrained molecular dynamics simulations. *J. Chem. Phys. 121*, 2904−2914.
(61) Hénin, J., Fiorin, G., Chipot, C., and Klein, M. L. (2010) Exploring multidimensional free energy landscapes using time-dependent biases on collective variables. *J. Chem. Theory Comput. 6*, 35−47.